RESEARCH ARTICLE | NOVEMBER 04 2025

Hosting capacity considerations for the combination of wind and solar on distribution electric power systems subject to different levels of coincident operations

C. Birk Jones ; Thad Haines ; Rachid Darbali-Zamora

J. Renewable Sustainable Energy 17, 066304 (2025)
https://doi.org/10.1063/5.0264545

Journal of Renewable and Sustainable Energy ARTICLE pubs.aip.org/aip/rse

Hosting capacity considerations for the combination of wind and solar on distribution electric power systems subject to different levels of coincident operations

Cite as: J. Renewable Sustainable Energy **17**, 066304 (2025); doi: 10.1063/5.0264545
Submitted: 11 February 2025 · Accepted: 5 October 2025 ·
Published Online: 4 November 2025

View Online Export Citation CrossMark

C. Birk Jones,[a] Thad Haines, and Rachid Darbali-Zamora

AFFILIATIONS

Renewable Distributed Systems Integration, Sandia National Laboratories, 1515 Eubank Blvd SE, Albuquerque, New Mexico 87123, USA

[a]Author to whom correspondence should be addressed: cbjones@sandia.gov

ABSTRACT

The integration of solar photovoltaic (PV) and wind turbine (WT) systems into distribution electric power systems presents challenges in steady-state operational performance (i.e., voltage and thermal loading) and capacity management, particularly under varying generation patterns. This study quantifies the interplay between PV and WT systems by first analyzing their time-series signal correlation coefficients over a full year of operation. These coefficients provide a basis for identifying locations with distinct PV–WT interaction patterns. Using Quasi-Static Time Series power flow simulations across representative locations and varying Distributed Energy Resource (DER) penetration levels, hosting capacity (HC) simulations then quantify the combined impacts of PV and WT. The simulation results indicate that correlation coefficients can serve as indicators of potential line loading trends but are less effective in anticipating voltage violations, underscoring the complexity of steady-state HC analysis. As expected, non-concurrent generation—wind at night and solar during the day—mitigates operational stress, though this behavior occurs only in limited U.S. locations. The outcomes from this methodology, when applied to specific territories and feeders, provide a systematic means of identifying representative locations and quantifying combined PV–WT HC impacts. These results can directly support integration planning, resource siting, and DER dispatch strategies.

I. INTRODUCTION

The integration of renewable energy resources into distribution electric power systems (EPS) presents significant challenges, particularly in managing grid stability, capacity, and operational variability.[1] To address these challenges, utilities conduct grid impact analyses during the interconnection permit stage to evaluate the effects of new distributed generation (DG) resources.[2,3] However, many studies analyze these systems in isolation, focusing on individual renewable technologies. This research bridges this gap by investigating the combined impacts of solar photovoltaic (PV) and wind turbine (WT) generators on EPS distribution grids.

While previous hosting capacity (HC) studies have extensively evaluated PV and WT systems independently,[4] few have explored their concurrent and non-concurrent behaviors under varying temporal and seasonal conditions on the same distribution grids. Furthermore, limited attention has been given to how different levels of coincident generation influence grid performance. These gaps are critical since realistic weather patterns, DG models, and Quasi-Static Time Series (QSTS) simulations provide a more accurate depiction of system interactions when PV and WT operate together.[5]

This study has two primary objectives:

1. Analyze the correlation between PV and WT outputs to characterize concurrent and non-concurrent generation behaviors.
2. Evaluate the combined impacts of PV and WT on grid performance across different times of the day and seasons under varying penetration levels and geographic locations.

To achieve these objectives, the study is structured into two key components: (1) an evaluation of WT and PV output signals and (2) a power grid impact analysis.

First, a correlation analysis, as described in a recent publication by the same authors,[6] computes a correlation coefficient® to quantify the alignment between PV and WT output signals at each location. Prior work used the R values to define WT and PV operational zones,[6] whereas this study extends that analysis to evaluate the grid impacts at locations with varying R values.

Evaluating grid impacts at every location across the U.S. would be computationally prohibitive. To address this, a clustering technique is applied to the R values to identify representative sites. The most representative sites (i.e., cluster centroids) are selected for power simulations to quantify grid impacts. These sites serve as proxies for regions with similar PV–WT correlation characteristics.

Second, the grid impact analysis employs QSTS simulations to evaluate different PV and WT penetration levels over a full year of operation. These simulations incorporate realistic weather and load profiles for each U.S. location, providing a comprehensive assessment of renewable energy impacts on the power grid. The results examine whether correlation analysis can serve as an indicator of potential grid impacts—such as voltage changes or line and transformer loading—under different PV–WT interaction patterns. While the feeder model is held constant in this study, the correlation values highlight renewable generation behaviors that can influence HC outcomes.

In summary, this paper details the methodology and presents a sample implementation using data from the Continental U.S. The results demonstrate the approach's effectiveness in assessing and quantifying the combined operations of PV and WT systems on distribution grids. By analyzing eight distinct operational scenarios, this study provides insights that utilities and policymakers can leverage to optimize energy dispatch strategies, enhance grid reliability, and support the efficient integration of DG resources.

II. BACKGROUND

Research on the integration of distributed PV and WTs into distribution EPS spans multiple topics, including grid performance, HC, and protection coordination.[7] Utilities rely on HC analyses and planning evaluations to mitigate potential disturbances.[8] To quantify the impact of distributed generation (DG) resources, researchers have developed deterministic, stochastic, and time-varying HC methodologies.[4,9]

Deterministic and static HC analyses assess power systems under predefined conditions, assuming constant load and generation levels. While these simulations provide valuable insights—such as identifying PV penetration limits based on voltage and current constraints[10]—they fail to account for uncertainties in weather variability, spatial distribution, and penetration levels.[11]

To address these limitations, probabilistic and scenario-based methods have been developed, incorporating uncertainty into DG integration analyses. These approaches consider fluctuations in PV and WT outputs,[12] with some employing advanced techniques such as Bayesian optimization to improve HC assessments.[13] Other studies explore the effects of varying DG placements and penetration levels, including applications like electric vehicles (EVs)[14] and PV systems.[15]

Time-varying assessments, particularly QSTS simulations, offer a more dynamic evaluation of load and generation variability. These simulations help identify critical operational challenges such as voltage unbalance and overloading, which are exacerbated by the simultaneous integration of PV and WT systems.[9,16]

PV and WT generators are often regarded as complementary energy sources, with PV systems providing peak output during daylight hours and WTs generating power at night. This temporal complementarity mitigates fluctuations in individual renewable outputs, reducing overall variability and enhancing grid performance and compliance.[17,18] While some studies have analyzed this complementarity using correlation techniques,[19,20] few have directly assessed its implications for power system performance.

A key challenge in evaluating the simultaneous integration of multiple Distributed Energy Resources (DERs) has been the availability of high-resolution spatial and temporal data. Recent advancements from the National Renewable Energy Laboratory (NREL) now provide extensive datasets that enable more detailed studies of hybrid PV and WT system implementations.[21] Despite these advancements, research on hybrid DER operations at the distribution grid level remains limited, particularly for small-scale PV and WT systems distributed across multiple locations. This study addresses this gap by leveraging advanced QSTS simulations and NREL's high-resolution data to assess the combined impacts of PV and WT systems on EPS performance.

Despite these advancements, research on hybrid DER operations at the distribution grid level remains limited, particularly for small-scale PV and WT systems distributed across multiple locations. Most HC methods either evaluate PV and WT in isolation or rely on exhaustive QSTS studies of all possible sites, which is computationally prohibitive. To address these deficiencies, this study introduces a correlation-based clustering methodology that identifies representative sites based on PV–WT interaction patterns. By jointly evaluating PV and WT generation in QSTS hosting capacity simulations, our approach captures interaction effects that isolated analyses overlook while substantially reducing computational effort. This enables utilities to more efficiently anticipate when combined resources exacerbate grid stress or provide complementary benefits, directly supporting planning and siting decisions.

III. ANALYSIS METHODOLOGY

This assessment is structured around two primary thrusts, illustrated in Fig. 1, which collectively aim to evaluate the combined impacts of PV and WT systems on distribution grids. The analysis begins by examining signal correlations between PV and WT outputs to characterize their concurrent and non-concurrent generation patterns. This step is critical for identifying temporal overlaps and their implications for grid performance while also guiding the selection of representative sites for simulation.

Using the correlation analysis results, a K-means clustering algorithm categorizes sites based on their distinct temporal generation behaviors. This categorization ensures that representative locations with unique PV and WT characteristics are selected, thereby minimizing redundant computational efforts. The selected profiles and penetration levels for PV and WT resources are then integrated into a grid simulation environment. Iterative simulations, which vary penetration levels, provide insights into the impacts of different concurrent patterns on hosting capacity, voltage stability, and grid reliability.

Sections III A–III C provide a detailed description of the methodology, including an overview of weather data (Subsection III A), analysis algorithms (Subsection III B), and hosting capacity simulations (Subsection III C). A demonstration use case implementation is presented in the results section to validate the methodology's effectiveness.

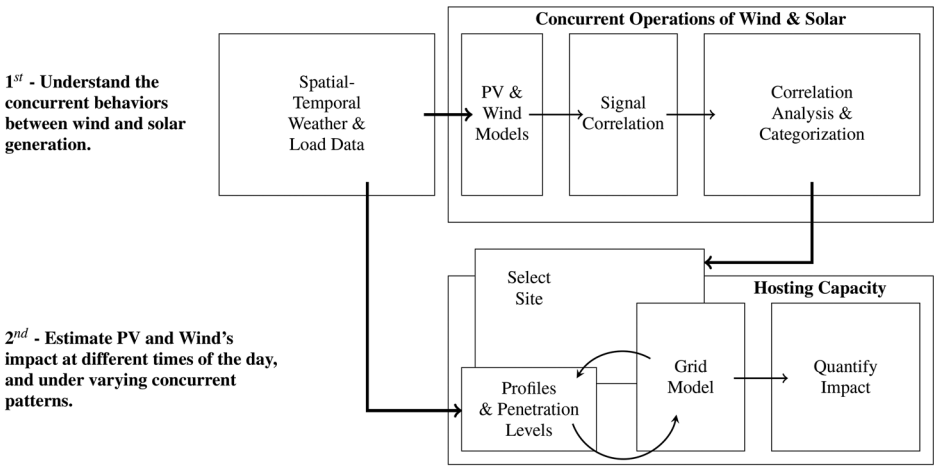

FIG. 1. Block diagram of the analysis methodology for estimating concurrent PV–WT operations and quantifying their combined impacts.

A. Spatial–temporal weather and load data

NREL's Highly Scalable Data Service (HSDS) provided access to the Wind Integration National Dataset (WIND),[22] offering wind resource information across the U.S. at a $2 \times 2\,\mathrm{km}^2$ spatial resolution and 1-h intervals. To reduce computational complexity while retaining sufficient spatial granularity, the dataset was down-sampled to a $60 \times 60\,\mathrm{km}^2$ resolution. This adjustment balances the need for detailed wind resource data with the feasibility of processing the large dataset.

Load data were sourced from *OpenEI's* End-Use Load Profiles for the U.S. Building Stock dataset,[23] which provides hourly demand profiles for residential, commercial, and industrial sectors across diverse climate zones. These load profiles were geographically matched to locations identified through the correlation clustering analysis, ensuring alignment between generation and demand patterns. By integrating these datasets, the study captures the spatial and temporal dynamics of renewable generation and grid consumption, enabling realistic simulations of grid impacts.

B. Concurrent operations of wind and solar

To evaluate the interaction between WT and PV systems, this study examines their generation signals using Pearson correlation analysis. The R quantifies the degree of synchronicity between these resources, with values categorized as positive ($R > 0$), negative ($R < 0$), or close to zero ($R \approx 0$). Positive correlations indicate simultaneous generation, which could exacerbate grid constraints, while negative correlations suggest complementary behavior that spreads generation to all hours of the day. Values near zero indicate that the two resources operate independently with minimal correlation.

1. Signal correlation

The simultaneous or non-simultaneous generation of electrical power from PV and WT systems significantly influences grid operations. PV systems produce power exclusively during daylight hours when sunlight is available, while WT systems can generate power during both day and nighttime hours. In summary, the potentially complementary behavior can expand local power generation to all hours of the day, or the wind power generation will coincide with solar output, depending on local meteorological conditions.

As a result, the integration of both PV and WT systems into distribution grids offers both opportunities and challenges. A key benefit is the diversification of renewable energy resources, reducing reliance on a single generation source. This combined operation may also smooth the inherent variability of each resource, leading to a more stable and predictable power generation signal. However, simultaneous generation can exacerbate grid challenges in regions with limited infrastructure, potentially causing thermal overloading and voltage levels that exceed American National Standards Institute (ANSI) limits,[24] risking damage to connected equipment.

To understand the interaction between wind and solar power, this study evaluates each time-series generation signal. The evaluation uses Python's NumPy correlation coefficient package,[25] which computes the Pearson correlation coefficient matrix, R, for the two one-dimensional arrays X (solar generation) and y (wind generation). The Pearson correlation coefficient is defined as

$$R = \frac{\mathrm{cov}(X, Y)}{\sigma_X \cdot \sigma_Y}, \tag{1}$$

where $\mathrm{cov}(X, Y)$ is the covariance between the time-series data X and Y, and σ_X and σ_Y are the standard deviations of X and Y, respectively. The covariance is calculated as

$$\mathrm{cov}(X, Y) = \frac{1}{n-1}\sum_{i=1}^{n}(X_i - \bar{X})(Y_i - \bar{Y}), \tag{2}$$

where n is the number of data points, X_i and Y_i are individual observations, and $\bar{X}$ and $\bar{Y}$ are the mean values of X and Y, respectively. The standard deviations, σ_X and σ_Y, are computed as

$$\sigma_X = \sqrt{\frac{1}{n-1}\sum_{i=1}^{n}(X_i - \bar{X})^2}, \qquad \sigma_Y = \sqrt{\frac{1}{n-1}\sum_{i=1}^{n}(Y_i - \bar{Y})^2}. \tag{3}$$

The resulting R values provide insights into the temporal relationship between PV and WT generation at different locations. The characterization breaks the R down into three categories:

1. Positive correlation ($R > 0$): Indicates that wind and solar generation tend to occur simultaneously, which may exacerbate grid impacts due to coincident power injections.
2. Negative correlation ($R < 0$): Suggests an inverse relationship, where wind and solar generation tend to occur at different times, potentially complementing each other and stabilizing grid operations.
3. No correlation ($R \approx 0$): Reflects a lack of a consistent relationship between wind and solar generation, with generation occurring both concurrently and non-concurrently.

2. Location correlation coefficient categorization

To perform a thorough evaluation while minimizing redundant simulations, this study employs a clustering approach to group locations with similar seasonal correlation behaviors. Specifically, the K-means++ clustering algorithm clusters locations based on their R for the four distinct seasons within a year.

The K-means algorithm was implemented in Python (scikit-learn),[26] which by default uses the K-means++ initialization method. This improves convergence reliability compared with purely random initialization. K-means++ is an unsupervised machine learning technique that partitions data points into clusters based on similarity. Here, each data point represents a geographic location, characterized by a four-dimensional feature vector containing seasonal R values.

Cluster quality was evaluated using both the elbow method (within-cluster sum of squares) and silhouette score analysis. The elbow method indicated diminishing returns beyond $k \approx 6$, while silhouette scores stabilized around 0.20–0.25 for $k = 4$–15. Based on these indicators, $k = 8$ was selected as a balance between capturing diverse seasonal correlation behaviors and maintaining computational tractability.

The clustering process begins by initializing k centroids as the initial cluster centers. Each data point (i.e., x_j) is then assigned to the nearest cluster based on the Euclidean distance to the centroids

$$C_i = \left\{ \boldsymbol{x}_j : ||\boldsymbol{x}_j - \mu_i||^2 \leq ||\boldsymbol{x}_j - \mu_l||^2 \, \forall \, l = 1, 2, \ldots, k \right\}, \tag{4}$$

where C_i represents the set of data points within cluster i, and μ_i is the centroid of cluster i. The algorithm then iteratively updates the centroids by computing the mean of all points assigned to each cluster

$$\mu_i = \frac{1}{|C_i|} \sum_{\boldsymbol{x}_j \in C_i} \boldsymbol{x}_j. \tag{5}$$

This iterative process continues until cluster assignments stabilize, minimizing the within-cluster sum of squared distances:

$$\text{minimize } J = \sum_{i=1}^{k} \sum_{\boldsymbol{x}_j \in C_i} ||\boldsymbol{x}_j - \mu_i||^2. \tag{6}$$

Once clustering is complete, the geographic location of each cluster centroid is identified and used for further analysis. The centroid represents the most typical or "average" site within its cluster, ensuring that the study captures diverse geographic and seasonal behaviors while maintaining computational efficiency. By grouping locations with similar seasonal R, this approach enables a detailed yet scalable assessment of wind and solar interactions across a large dataset, providing a solid foundation for subsequent HC simulations.

C. Hosting capacity simulations

The HC simulations estimate the impact of PV and WT systems at different times of the day and under various concurrent operational patterns based on the location's weather. Figure 1 illustrates this process, which involves selecting representative sites, gathering input data, and defining DER penetration levels. These grid simulations evaluate the effects of different penetration levels on voltage stability, line loading, and other performance metrics under diverse operational scenarios.

This study considers the impact on the distribution feeder model kept fixed across the test locations, while the PV and WT generation profiles vary. The clustering process is therefore applied solely to group locations with similar PV–WT correlation characteristics, reducing the number of representative sites to be simulated. The approach does not attempt to capture diversity in feeder topologies but instead focuses on how temporal resource interactions influence hosting capacity on a fixed feeder.

1. Site selection

The site selection process leverages the representative locations identified in the clustering step (Sec. III B 2). These centroids capture distinct seasonal PV–WT correlation behaviors, allowing the simulations to efficiently evaluate grid impacts across diverse resource interaction patterns while minimizing computational redundancy. Additional scope assumptions, including clarification that the distribution feeder model is held constant across all locations.

2. Input profiles and resource penetration levels

The HC simulations require weather profiles, load profiles, and DER penetration levels, as depicted in the "Profiles & Penetration Levels" block of Fig. 1.

Weather profiles for each selected site are obtained from the NREL WIND[22] and National Solar Radiation Database (NSRDB)[28] datasets, providing hourly wind speed, irradiance, and temperature data for a full year. Hourly load data from the OpenEI platform[23] capture residential, commercial, and industrial demand patterns, ensuring realistic grid consumption behavior. Penetration levels range from low to high adoption scenarios, systematically applied to load locations within the grid model.

3. Grid model hosting capacity simulations

The HC simulations use the SMART-DS distribution system model,[33] implemented in OpenDSS.[32] The grid model integrates site-specific weather and load data before configuring PV and WT systems at varying penetration levels. Once the setup is complete, the HC simulation proceeds as follows:

1. Assign DER penetration levels: PV and WT systems are allocated to load nodes according to predefined penetration scenarios. The spatial locations and sizes of DERs were initialized in this step and then held constant across all simulations, ensuring that

differences in hosting capacity outcomes arose solely from PV–WT generation profiles rather than changes in siting.
2. Run QSTS simulations: A full year of QSTS simulations captures seasonal and hourly variations in generation and consumption.
3. Analyze grid performance metrics: Voltage levels, line loading, and other key performance indicators are evaluated to identify potential violations of ANSI voltage standards and thermal limits.

4. Hypothesis testing

These simulations test whether grid impacts depend on the correlation between PV and WT generation, with different expectations based on correlation type.

1. Positive correlation: Locations with simultaneous generation are expected to exhibit the highest frequency of voltage violations and thermal overloads due to coincident power injections.
2. Negative correlation: Locations with complementary generation are hypothesized to experience fewer issues, as generation patterns naturally balance each other.
3. No correlation: Locations with uncorrelated generation may display intermediate levels of impact, as simultaneous and non-simultaneous generation patterns occur sporadically.

By systematically analyzing these scenarios, this study quantifies the relationship between PV–WT correlation and grid hosting capacity, providing insight into potential operational constraints and opportunities for optimizing DER integration.

IV. DEMONSTRATION ASSESSMENT

A demonstration assessment of WT and PV systems across the U.S. evaluates the methodology's effectiveness in analyzing and quantifying grid impacts. This assessment consists of two interconnected components: (1) a concurrent operations analysis to identify temporal generation patterns and (2) hosting capacity simulations to assess grid impacts under varying scenarios. Table I summarizes the datasets used in this evaluation.

The case study spans a full year of operations across the Continental U.S., using representative locations to balance computational efficiency with comprehensive geographic coverage. By selecting this subset of sites, the analysis ensures that diverse wind and solar generation characteristics are captured, enabling a detailed evaluation of how different levels of wind–solar correlation influence grid hosting capacity.

A. Wind and solar power system simulations

This study models WT power generation using Python's *windpowerlib*,[30] a widely used library for simulating wind energy systems.[34] WT power output is estimated based on the power curve of a Bergey Excel 10 8.9 kW turbine.[35] The power curve defines the relationship between wind speed and power generation, enabling accurate simulation of WT behavior under diverse wind conditions.

PV power generation is simulated using NREL's PVWatts model, implemented in Python's PVLIB package.[36] This model accurately predicts grid-connected PV performance using real-world solar radiation and temperature data.[29] The direct current (DC) power (P_{DC}) output is computed using the following equation:

$$P_{dc} = \frac{G_{poa}}{1000} P_{dc0}(1 + \gamma_{pdc}(T_{cell} - T_{ref})), \quad (7)$$

where G_{poa} is the plane-of-array irradiance (W/m^2), T_{cell} is the module temperature, T_{ref} is the reference temperature (25 °C), P_{dc0} is the system's nameplate DC rating, and γ_{pdc} is the temperature coefficient (1/°C). To ensure consistency in grid simulations, the PV system's capacity was set to 8.9 kW, matching that of the simulated WT.

B. Correlation categorization

Using the WT and PV models described above, simulations were conducted for locations across the Continental U.S. R values were computed for each location across the four seasons: winter, spring, summer, and fall. These seasonal correlations, shown in Fig. 2, highlight the temporal relationships between wind and solar power generation.

1. Correlation results

The heatmaps in Fig. 2 illustrate the spatial variations in PV and WT generation signals. Blue regions indicate negative correlations, where PV and WT generation tend to occur at different times, while red regions indicate positive correlations, signifying simultaneous generation. Key observations of these heatmaps include:

1. Winter and fall: Negative correlations dominate, especially in western regions, indicating that wind and solar generation often occur at different times.
2. Spring and summer: Positive correlations are more prevalent, particularly in the Midwest and Eastern states, where concurrent PV and WT generation is common.
3. Western U.S.: While negative correlations are frequent throughout the year, the magnitudes are generally small, suggesting that non-concurrent generation is not strongly pronounced.

These spatial and temporal variations emphasize the importance of understanding concurrent and non-concurrent generation patterns when integrating PV and WT systems into distribution grids.

2. Clustering analysis results

To streamline the analysis and reduce computational demands, a K-means++ clustering algorithm was applied to group locations based on their seasonal R. Clustering was performed using these seasonal R values as input features, represented as

```
{"feature 1": "R_winter",
 "feature 2": "R_spring",
 "feature 3": "R_summer",
 "feature 4": "R_fall"}
```

The clustering process produced eight distinct categories, which are visualized in Fig. 3. The choice of eight clusters was supported by both elbow and silhouette analyses, which showed diminishing returns in within-cluster variance reduction beyond k ≈ 6 and stable silhouette values across k = 4–15. Each category groups locations with

TABLE I. Data used to achieve the two objectives.

No.	Objective type	Wind data	Weather data	Load data	PV model	WT model	Grid model
1	Concurrent operations	NREL Wind Resource Database[27]	National Solar Radiation Database (NSRDB)[28]	N/A	PVWatts[29]	windpowerlib[30]	N/A
2	Hosting capacity	NREL Wind Resource Database[27]	National Solar Radiation Database (NSRDB)[28]	Open Energy Data Initiative (OEDI)[31]	OpenDSS[32]	OpenDSS[32]	SMART-DS[33]

similar seasonal correlation behaviors, ensuring that diverse geographic and temporal patterns are represented. To further reduce computational effort, the centroid (μ) of each cluster was selected as the representative site for subsequent hosting capacity simulations. These representative locations, labeled A–H in Fig. 3, encompass a wide range of operating conditions across the U.S.

The seasonal PV vs WT R for the representative sites are summarized in Table II. Each row describes the K-means cluster category, the corresponding location (labeled A–H in Fig. 3), and the computed signal correlation values for each season. This table provides detailed insights into the correlation patterns at each location:

1. Positive correlations: Locations such as A and D exhibit higher positive R values during spring and summer, indicating frequent concurrent generation.
2. Negative correlations: Locations like G and H demonstrate negative correlations, particularly in summer, when wind and solar generation often occur at different times.
3. Mixed patterns: Some locations, such as B and C, show a mix of positive and near-zero correlations, reflecting variability in seasonal generation behaviors.

These representative sites capture the diversity of correlation behaviors, providing a robust basis for evaluating grid impacts under different generation patterns.

C. Electric power grid models

The electric power grid model used in this study, shown in Fig. 4, represents a residential feeder system. This model is part of the SMART-DS repository,[33] a collection of synthetic grid models designed to replicate real-world distribution networks. For this demonstration, the Santa Fe feeder model, designated as "$uhs_0$1247–udt4776," The feeder designation is taken directly from the SMART-DS file set corresponding to Santa Fe, NM. To avoid confusion, this simulation effort used the exact alphanumeric feeder identifier as provided in the dataset files.

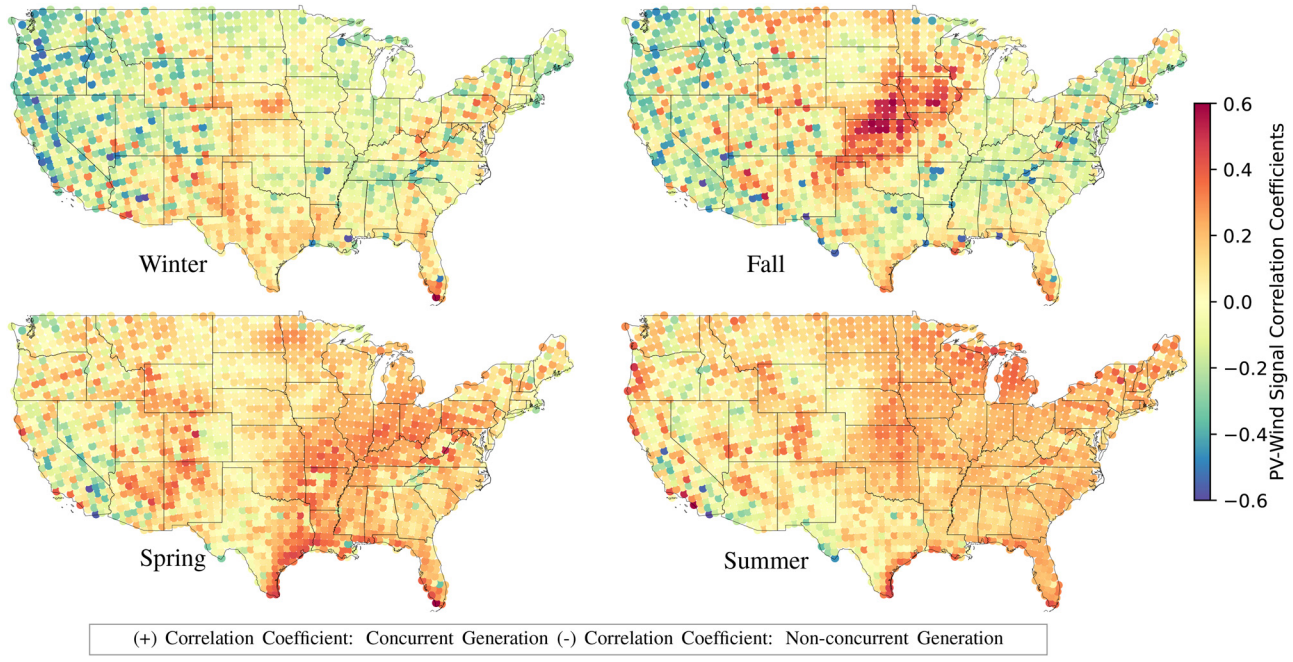

FIG. 2. Seasonal correlation coefficients® of PV and wind generation. Positive values indicate concurrent generation, negative values indicate non-concurrent generation, and near-zero values indicate mixed patterns.

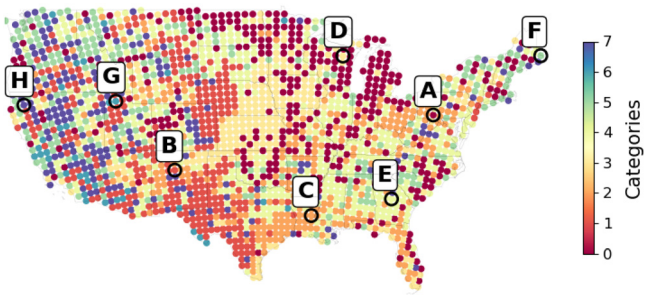

FIG. 3. Heatmap of the eight signal correlation categories. Alphabetic labels denote the locations of category centroids, which correspond to the sites used in the demonstration experiment.

The feeder model includes a substation (bottom left of Fig. 4) that connects the distribution network to the transmission grid, which is modeled as an infinite source to ensure a stable power supply. The distribution system serves 1746 primarily residential loads, with a total peak demand of 9868 kW and an average maximum load per customer of 5.65 kW.

To support voltage regulation, the system includes two capacitors rated at 12.47 kV with capacities of 600 and 450 kvar. Additionally, 601 transformers connect the primary distribution lines to lower-voltage secondary lines, ensuring compatibility with residential load requirements. These components contribute to a realistic test scenario for quantifying and comparing the impacts of wind and solar integration on distribution grid performance.

With this distribution system model established, the next step involves defining the input datasets that characterize demand, renewable generation, and penetration scenarios.

D. Model inputs—profiles and penetration levels

To evaluate the grid impacts of PV and WT integration under varying conditions, the simulations incorporate a full year of demand and weather data. These inputs enable an in-depth analysis of the temporal dynamics of renewable generation and demand across different scenarios.

Figure 5 summarizes the demand, PV generation, and WT output profiles, displaying their hourly variations throughout the year. Locations A and D, which exhibit relatively high positive R, demonstrate concurrent generation patterns, as shown in the figure. In contrast, location 6, with the largest negative R value, highlights complementary behavior, with WT generation peaking at night and PV generation occurring during daylight hours.

TABLE II. Seasonal PV vs wind signal correlations.

Category	Location	Winter	Spring	Summer	Fall
0	A	0.1238	0.2151	0.2338	0.1166
1	B	0.1737	0.1139	0.0140	0.1190
2	C	0.2072	0.2877	0.1487	0.1295
3	D	0.1757	0.2117	0.2584	0.2203
4	E	0.1434	0.1906	0.1390	0.0792
5	F	0.032 11	0.091 05	0.1142	0.018 61
6	G	0.050 01	−0.067 23	−0.2343	−0.037 59
7	H	0.014 76	0.006 370	−0.059 95	−0.041 49

1. Integration scenarios

This study evaluates four integration scenarios to quantify the grid impacts of varying PV and WT deployment levels. Table III summarizes the number of PV and WT systems deployed under each scenario. For each simulation, the DER sites remain constant.

2. Resource placement

When assigning resources to the grid, PV and WT system sizes were distributed to reflect real-world deployment patterns. The PV system sizes were assigned as follows: 5% at 3 kW, 10% at 4 kW, 35% at 5 kW, 35% at 6 kW, and 25% at 10 kW. Similarly, WT system sizes were distributed as 5% at 5 kW, 60% at 10 kW, and 35% at 20 kW.

PV and WT systems were randomly assigned once across the grid, with some co-located at the same load/bus to reflect real-world variability in DER deployment. This initialization was held constant in all subsequent scenarios, ensuring that differences in hosting capacity outcomes arose from PV–WT generation profiles rather than changes in DER siting. By incorporating realistic demand profiles, weather data, and variable penetration levels, this methodology establishes a robust framework for evaluating the grid impacts of renewable energy integration.

By incorporating realistic demand profiles, weather data, and variable penetration levels, this methodology establishes a robust framework for evaluating the grid impacts of renewable energy integration.

E. Simulation grid impacts

The integration of PV and WT power generation significantly impacts electric grid performance, with effects varying based on the time of day and specific geographic location. These impacts are

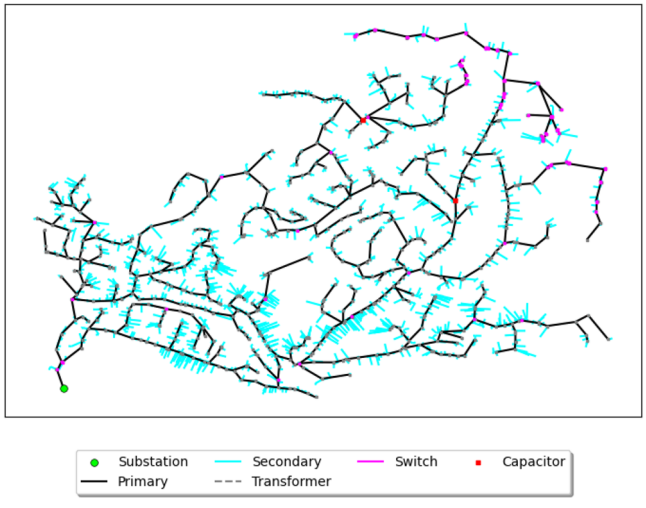

FIG. 4. Topological map of the distribution electric power system model used in the hosting capacity assessment demonstration.

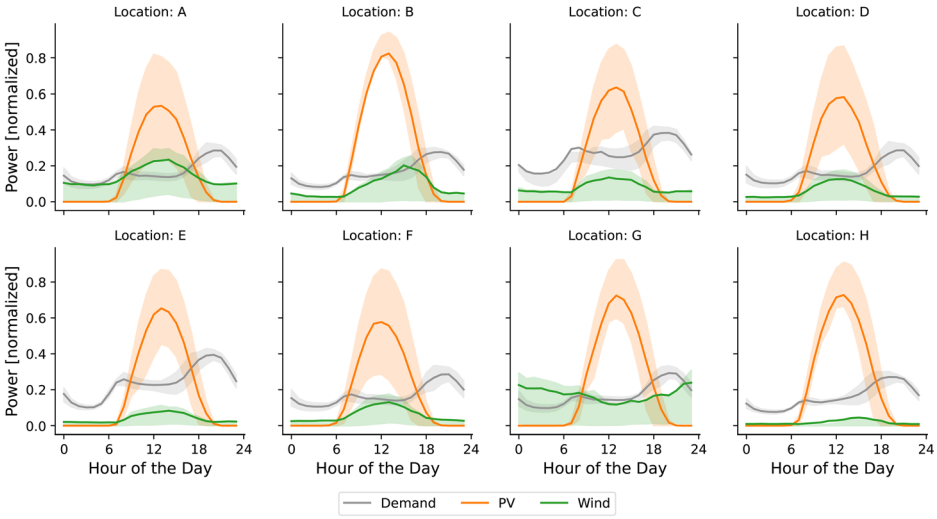

FIG. 5. Normalized demand, PV generation, and wind power output for the eight locations. Solid lines show the median hourly values, and shaded regions indicate the 25th–75th percentile ranges.

TABLE III. PV and wind integration scenarios.

Type	Scenario 0	Scenario 1	Scenario 2	Scenario 3
PV	0	436	872	1500
Wind	0	170	340	694

primarily reflected in three key metrics: voltage, line loading, and transformer loading.

The following subsections discuss the hourly results for voltage impact (Subsection IV E 1), line loading (Subsection IV E 2), and transformer loading impacts (Subsection IV E 3), highlighting the temporal variations in grid performance across different scenarios. The power system impacts of PV and WT generation vary throughout the day, as illustrated in Figs. 6–8. These figures depict the progression of voltage, line loading, and transformer loading across four scenarios, from scenario 0 (no PV or WT systems) to scenario 3 (highest penetration levels). In each plot, the solid lines represent the mean profile over the year, while the shaded regions indicate the 25th and 75th percentiles.

The joint PV–WT analysis moves beyond current practice, where PV and WT integrations are typically studied in isolation. Prior PV-only studies would attribute most daytime voltage rise to solar generation; our results show that concurrent wind output compounds this effect. Conversely, PV-only studies would miss the benefits of negative correlations, where nighttime wind complements daytime PV, enabling a more continuous distribution of power generation across a full 24-h period. By evaluating PV and WT together, this study demonstrates interaction effects that are not visible in isolated analyses, reinforcing the importance of accounting for coincident and non-coincident resource behavior in hosting capacity assessments.

1. Voltage impacts

Figure 6 shows the typical daily voltage profiles for each scenario at all locations over the full year.

1. Scenario 0 (baseline): Voltage remains relatively stable around 1.03 per unit (PU).
2. Scenario 1 (initial integration): Voltage increases during daylight hours caused by PV generation, rising to approximately 1.04 PU.
3. Scenario 2 (medium integration): Voltage increases above the initial integration scenario but remains below the ANSI limit of 1.05 PU.
4. Scenario 3 (high penetration): Voltage further increases, exceeding 1.05 PU in some cases, particularly during peak PV production hours.

The results suggest that voltage changes closely follow PV power generation. Each location (A–H) experiences a voltage "hump" during daytime hours, corresponding to typical PV production as shown in Fig. 5. WT impacts are less apparent but can be seen during the early morning hours (between hours 0 and 6). In locations where more WT power production occurs at night, such as location G (which had a negative R value when comparing the WT and PV output signals), the increase in voltage from scenario 0 to 3 is most apparent.

2. Line loading impacts

Figure 7 provides a statistical review of the daily line loading profiles for the secondary lines in the distribution power grid. Observations show the following:

1. Scenario 0: As expected, line loading closely follows the demand profile, with minimal variability.
2. Scenarios 1–3: PV and WT generation significantly increase line loading during their production hours, with progressive increases observed across scenarios. During the night hours, the line-loaded increases due to wind power generation were very small in comparison to the daytime changes.

At locations G and H, which exhibit the most negative R values, line loading during daylight hours is lower than other locations. This is particularly evident in scenario 2, where non-concurrent operation of PV and WT mitigates the change rate in line loading.

3. Transformer loading impacts

Transformer loading impacts, shown in Fig. 8, closely follow the trends observed in the line loading results. Key observations include:

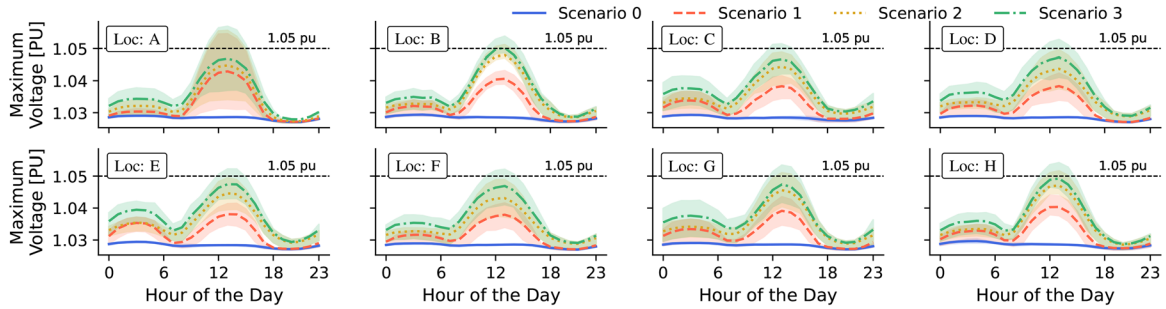

FIG. 6. Voltage profiles for each location and scenario. (The line represents the average, and the bounds describe the 25% and 75% quantiles.)

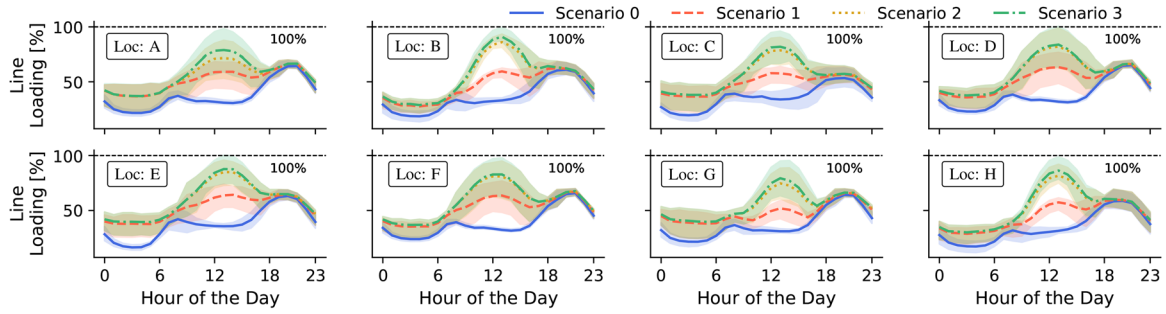

FIG. 7. Line loading for each location and scenario. (The line represents the average, and the bounds describe the 25% and 75% quantiles.)

1. Daytime peaks: Transformer loading peaks during PV generation hours, reflecting the additional power flowing through the transformers.
2. Non-concurrent benefits: Locations G and H, with negative R values, experience reduced transformer loading compared to locations with concurrent PV and WT generation.

This demonstrates the advantages of non-concurrent generation patterns, which help balance grid loading and reduce stress on critical components.

4. Impacts summary

The impacts of PV and WT generation on grid performance reveal distinct patterns across voltage, line loading, and transformer loading. PV generation has a pronounced influence on daytime voltage levels, while WT impacts are more noticeable at night, particularly in locations with negative R values. Increased penetration of PV and WT systems raises line loading, though this effect is mitigated in locations where their generation patterns are non-concurrent. Similarly, transformer loading follows trends observed in line loading, with reduced stress on transformers in areas where PV and WT generation complement each other temporally (i.e., operate at different times of day). These findings highlight the critical role of understanding and leveraging the temporal relationships between PV and WT generation to enhance grid performance and ensure system reliability.

F. Correlation coefficient pattern observations

A deeper analysis of the relationship between concurrent and non-concurrent WT and PV operations reveals connections between

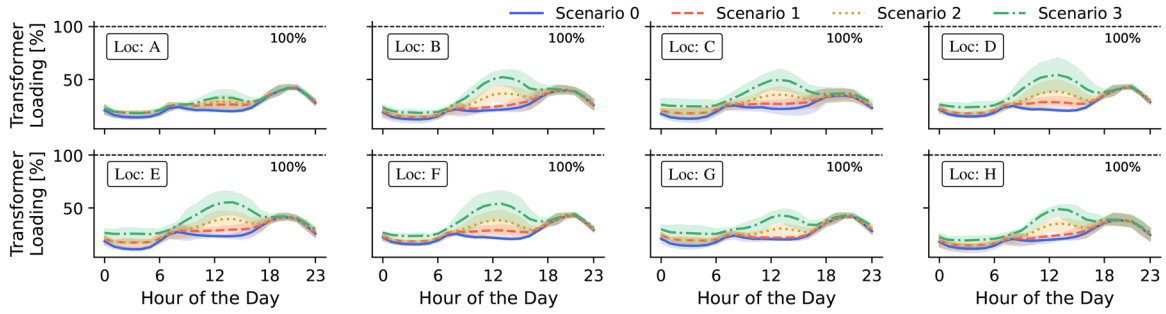

FIG. 8. Transformer loading at locations and scenarios. (The line represents the average, and the bounds describe the 25% and 75% quantiles.)

the mean R value and various grid performance metrics, including voltage, line loading, and transformer loading. Figures 9–11 illustrate these relationships across the three scenarios, focusing on the eight representative locations identified in Sec. III B 2.

The trend lines in Figs. 9–11 were generated using a least squares linear fit across scenario results. These are included to highlight the general direction of change with increasing DER penetration, rather than to imply precise predictive capability.

1. Voltage performance

Although some indications of a trend exist, the relationship between R and voltage performance, depicted in Fig. 9, lacks consistency. Key observations and insights include the following:

1. Average maximum voltage: Voltage remains relatively stable across the range of R values, indicating that concurrent or non-concurrent generation has minimal influence on this metric.
2. Over-voltage occurrences: In scenario 3, a slight decrease in over-voltage occurrences is observed as R becomes more positive, suggesting that higher PV and WT penetration levels may benefit from complementary generation patterns. However, this trend is not evident in lower penetration scenarios. Thus suggesting that high penetration levels benefit more from concurrent operations than when limited resources are integrated on a distribution grid.

These observations suggest that voltage behavior is less directly affected by the correlation between PV and WT generation compared to transformer and line loading metrics.

2. Line loading performance

Line loading metrics, shown in Fig. 10, display a stronger dependence on R than voltage. A review of the plots in Fig. 10 identifies the following:

1. Average line loading: A clear trend emerges, with average line loading increasing as R becomes more positive, reflecting higher stress during concurrent generation periods.
2. Maximum line loading: While the relationship is less pronounced for maximum line loading, the number of daily overloads (line loading exceeding 100%) correlates strongly with R. This is particularly evident in higher PV penetration scenarios (e.g., scenario 3), where greater concurrent generation significantly increases the likelihood of line overloading.

These findings highlight the critical role of managing concurrent generation patterns to mitigate the risk of line overloading in distribution networks.

3. Transformer loading performance

Figure 11 shows the relationship between R and two transformer loading metrics: average loading and the daily occurrence of transformer overloads (loading exceeding 100%). Critical insights include the following from each of the two plots in Fig. 11.

1. Average transformer loading: As R becomes more positive, average transformer loading increases across all three scenarios, indicating that concurrent generation from PV and WT systems places greater stress on transformers.
2. Overload occurrences: The number of overload occurrences does not exhibit a clear trend with R, possibly due to the limited frequency of overloads in the modeled scenarios.

These results suggest that transformer performance is sensitive to concurrent PV and WT operations, emphasizing the need to account for correlation effects in transformer capacity planning.

4. Correlation coefficient pattern summary

This analysis underscores the importance of understanding the interplay between PV and WT generation patterns. Positive R values, reflecting concurrent generation, are associated with higher average loading and a greater risk of overloads for both transformers and lines. In contrast, locations with negative R values, indicating complementary generation, experience reduced grid stress. While voltage impacts appear less sensitive to generation correlations, they remain an important consideration for grid operations performance at higher DER penetration levels. These insights provide guidance for optimizing DER deployment and managing grid impacts effectively.

Because clustering is based on centroids, the most extreme correlations were not represented among the selected sites. The results therefore emphasize typical correlation ranges ($R \approx -0.1$ to 0.25).

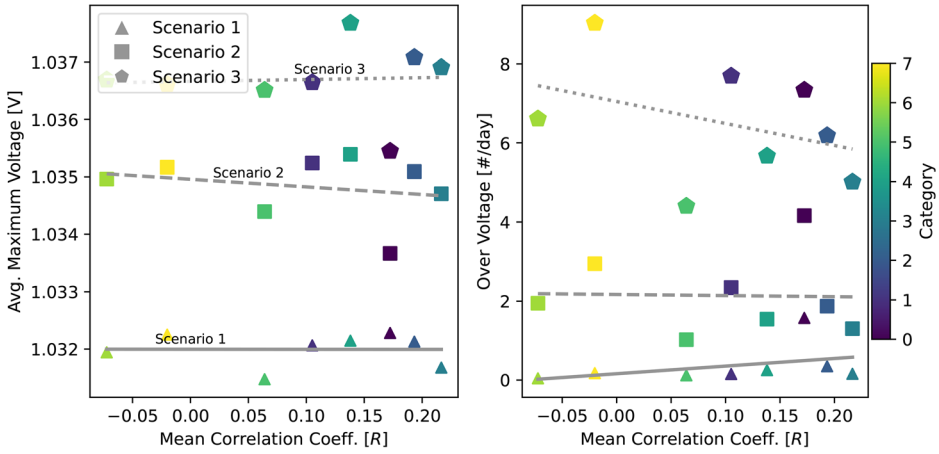

FIG. 9. Scatter plot comparing PV vs WT correlation coefficient® with respect to the two over-voltage metrics. Trend lines represent least squares linear fits included to indicate general directionality.

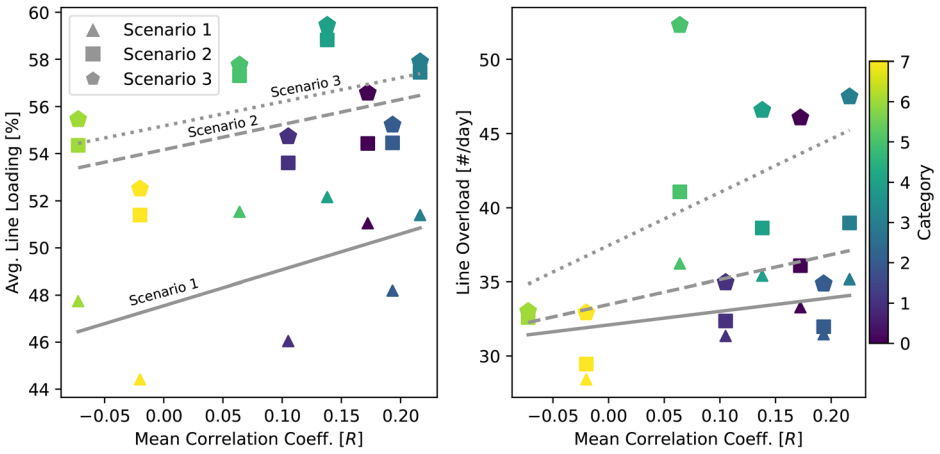

FIG. 10. Scatter plot comparing PV vs WT correlation coefficient[R] with respect to the two line loading metrics. Trend lines represent least squares linear fits included to indicate general directionality.

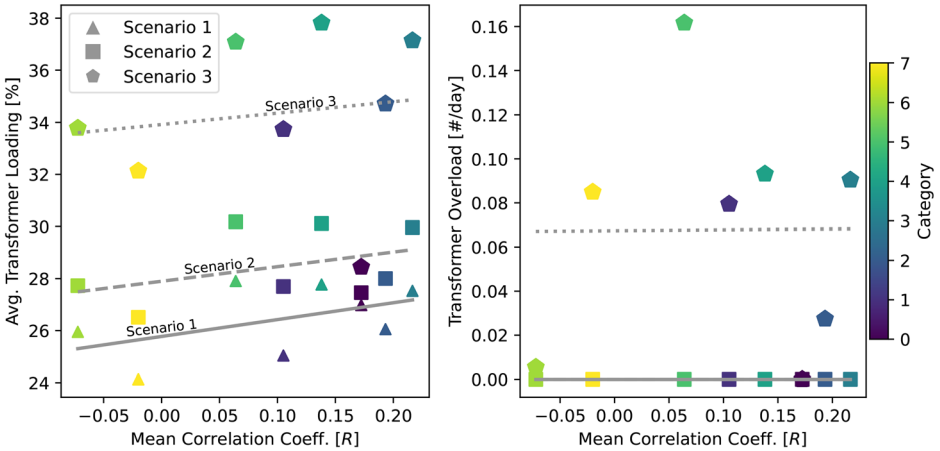

FIG. 11. Scatter plot depicting the relationship between transformer percent loading and overloads per day with the PV vs WT correlation coefficient[R]. Trend lines represent least squares linear fits included to indicate general directionality.

While the same general behaviors are expected at more extreme values, assessing those cases directly is left for future work.

V. CONCLUSIONS

This paper presented a novel methodology to assess the concurrent and non-concurrent operations of distributed solar photovoltaic (PV) and wind turbine (WT) generation on distribution electric power systems (EPS). As renewable energy integration accelerates to support decarbonization goals, understanding the operational dynamics of these resources becomes critical for maintaining grid reliability. This study addressed a gap in existing research by focusing on the interplay between PV and WT generation, which has often been analyzed independently.

Using signal correlation analyses, this research quantified the coincident and non-coincident generation patterns of PV and WT systems across different locations and seasons. These patterns were classified using a K-means clustering approach, enabling the identification of representative sites for HC simulations. The results revealed that locations with higher positive correlations between PV and WT generation experience greater impacts on voltage levels, line loading, and transformer loading. Conversely, areas with negative correlations benefit from reduced thermal stress, as PV and WT generation occur at complementary times.

Importantly, this study highlights the added value of evaluating PV and WT jointly rather than in isolation. While PV-only hosting capacity studies capture daytime voltage rise, our analysis shows that concurrent PV–WT operation can exacerbate these effects, whereas non-concurrent operation can mitigate them by spreading generation more evenly across a 24-h cycle. These findings demonstrate interaction effects not visible in isolated analyses, underscoring the need to incorporate coincident and non-coincident resource behavior into future hosting capacity assessments.

Key contributions of this work include:

1. Quantification of concurrent behaviors: Development of a methodology to analyze the temporal interactions between PV and WT generation using correlation analysis.
2. Categorization of locations: A streamlined approach for identifying representative sites, reducing the need for exhaustive simulations across all locations.
3. Impacts on grid performance: Insights into the combined effects of PV and WT generation on voltage stability and thermal loading.
4. Value of non-concurrent patterns: Demonstration of the benefits of complementary PV and WT generation in mitigating grid stress.

5. Actionable insights: By linking PV–WT correlation patterns to grid outcomes, this work provides utilities with a systematic way to identify representative study sites, anticipate where combined resources may exacerbate or alleviate grid stress, and design more efficient hosting capacity studies. For policymakers, the findings highlight how resource diversity and non-concurrent operation can enhance integration potential, informing siting strategies, interconnection standards, and infrastructure investment decisions.

These findings offer utilities and policymakers valuable insights into the dynamic behavior of renewable energy systems. By understanding how PV and WT systems interact, grid operators can make informed decisions to optimize grid reliability and support sustainable energy growth.

While the study provides significant insights, it is not without limitations. The analysis focused on specific demonstration cases within the Continental U.S. and utilized a single power grid model, which may not fully capture variations in weather patterns, grid configurations, or operational constraints in other regions. Additionally, the simulations did not incorporate advanced grid control technologies or energy storage systems, which could further mitigate some of the observed operational challenges.

Other limitations include the meteorological input data—solar irradiance and wind speed are inherently stochastic. While clustering captures typical seasonal correlation patterns, extreme events where PV and wind generation simultaneously reach maxima or minima may not be fully represented by the centroids. These rare coincidences could impose additional grid stress beyond the representative cases studied here. Future work could explicitly evaluate the impact of such joint extremes.

Future research directions include:

1. Expanding the methodology to other distributed generation types, such as battery storage or electric vehicles.
2. Investigating the role of advanced grid technologies in enhancing hosting capacity and mitigating grid impacts.
3. Applying the approach to larger and more diverse geographical regions to explore scalability and adaptability.
4. Analyzing the implications of higher renewable penetration levels in existing grid infrastructures.

In conclusion, this study underscores the critical role of concurrent and non-concurrent renewable generation patterns in shaping the operational dynamics of distribution grids. As the penetration of Distributed Energy Resources continues to grow, the methodology presented here provides a vital framework for maintaining grid stability while enabling the responsible integration of renewable energy. By leveraging these insights, utilities and policymakers can pave the way for a more reliable, resilient, and sustainable energy future.

ACKNOWLEDGMENTS

This article has been authored by an employee of National Technology & Engineering Solutions of Sandia, LLC under Contract No. DE-NA0003525 with the U.S. DOE. The employee owns all right, title, and interest in and to the article and is solely responsible for its contents. The U.S. Government retains, and the publisher, by accepting the article for publication, acknowledges that the U.S. Government retains a non-exclusive, paid-up, irrevocable, worldwide license to publish or reproduce the published form of this article or allow others to do so for U.S. Government purposes. The DOE will provide public access to these results of federally sponsored research in accordance with the DOE Public Access Plan.

The authors would like to acknowledge the financial support provided by the U.S. DOE, Office of Energy Efficiency (EERE), Wind Energy Technology Office (WETO) as part of the Interconnection Innovation e-Xchange (i2x) program as well as the contributions from Bret Barker and Patrick Gilman.

AUTHOR DECLARATIONS

Conflict of Interest

The authors have no conflicts to disclose.

Author Contributions

C. Birk Jones: Conceptualization (equal); Data curation (equal); Formal analysis (equal); Methodology (equal); Validation (equal); Visualization (equal); Writing – original draft (equal); Writing – review & editing (equal). **Thad Haines:** Formal analysis (supporting). **Rachid Darbali-Zamora:** Funding acquisition (lead); Writing – review & editing (supporting).

DATA AVAILABILITY

Data sharing is not applicable to this article as no new data were created or analyzed in this study.

REFERENCES

[1]A. Sajadi, L. Strezoski, V. Strezoski, M. Prica, and K. A. Loparo, "Integration of renewable energy systems and challenges for dynamics, control, and automation of electrical power systems," WIREs Energy Environ. **8**, e321 (2019).
[2]L. K. L. Estorque and M. A. A. Pedrasa, "Utility-scale DG planning using location-specific hosting capacity analysis," in *2016 IEEE Innovative Smart Grid Technologies—Asia (ISGT-Asia)* (IEEE, 2016), pp. 984–989.
[3]E. Mulenga, M. H. J. Bollen, and N. Etherden, "A review of hosting capacity quantification methods for photovoltaics in low-voltage distribution grids," Int. J. Electr. Power Energy Syst. **115**, 105445 (2020).
[4]V. de Cillo Moro, R. S. Bonadia, and F. C. L. Trindade, "A review of methods for assessing DER hosting capacity of power distribution systems," IEEE Lat. Am. Trans. **20**, 2275–2287 (2022).conference Name: IEEE Latin America Transactions.
[5]M. J. Reno, J. Deboever, and B. Mather, "Motivation and requirements for quasi-static time series (QSTS) for distribution system analysis," in *2017 IEEE Power & Energy Society General Meeting* (IEEE, 2017), pp. 1–5.
[6]C. B. Jones, G. Fragkos, and R. Darbali-Zamora, "Exploring the interplay between distributed wind generators and solar photovoltaic systems," J. Renewable Sustainable Energy **17**, 016104 (2025).
[7]M. Rylander, L. Rogers, and J. Smith, "Distribution feeder hosting capacity: What matters when planning for DER?" Technical Report No. 3002004777 (Electric Power Research Institute, 2015).
[8]J. Smith, M. Rylander, M. J. Reno, R. J. Broderick, B. Mather, J. E. Quiroz, and K. Munoz-Ramos, "Alternatives to the 15% rule: Modeling and hosting capacity analysis of 16 feeders," Technical Report No. SAND-2015-7450R (Sandia National Laboratories (SNL-NM), Albuquerque, NM, 2015).
[9]D. Diaz, A. Kumar, J. Deboever, S. Grijalva, J. Peppanen, M. Rylander, and J. Smith, "Scenario-selection for hosting capacity analysis of distribution feeders with voltage regulation equipment," in *2019 IEEE Power & Energy Society Innovative Smart Grid Technologies Conference (ISGT)* (IEEE, 2019), pp. 1–5.

[10]R. A. Shayani and M. A. G. de Oliveira, "Photovoltaic generation penetration limits in radial distribution systems," IEEE Trans. Power Syst. **26**, 1625–1631 (2011).
[11]A. Koirala, T. Van Acker, R. D'hulst, and D. Van Hertem, "Hosting capacity of photovoltaic systems in low voltage distribution systems: A benchmark of deterministic and stochastic approaches," Renewable Sustainable Energy Rev. **155**, 111899 (2022).
[12]H. Al-Saadi, R. Zivanovic, and S. F. Al-Sarawi, "Probabilistic hosting capacity for active distribution networks," IEEE Trans. Ind. Inf. **13**, 2519–2532 (2017).
[13]X. Geng, L. Tong, A. Bhattacharya, B. Mallick, and L. Xie, "Probabilistic hosting capacity analysis via Bayesian optimization," in *2021 IEEE Power & Energy Society General Meeting (PESGM)* (IEEE, 2021), pp. 1–5.
[14]C. B. Jones, M. Lave, and R. Darbali-Zamora, "Overall capacity assessment of distribution feeders with different electric vehicle adoptions," in *2020 IEEE Power & Energy Society General Meeting (PESGM)* (IEEE, 2020), pp. 1–5.
[15]F. Ding and B. Mather, "On distributed PV hosting capacity estimation, sensitivity study, and improvement," IEEE Trans. Sustainable Energy **8**, 1010–1020 (2017).conference Name: IEEE Transactions on Sustainable Energy.
[16]D. Schwanz, F. Moller, S. K. Ronnberg, J. Meyer, and M. H. J. Bollen, "Stochastic assessment of voltage unbalance due to single-phase-connected solar power," IEEE Trans. Power Delivery **32**, 852–861 (2017).
[17]A.-K. Gerlach, D. Stetter, J. Schmid, and C. Breyer, "PV and wind power – Complementary technologies," in *26th European Photovoltaic Solar Energy Conference and Exhibition* (WIP, 2011), pp. 4607–4613.
[18]A. A. Prasad, R. A. Taylor, and M. Kay, "Assessment of solar and wind resource synergy in Australia," Appl. Energy **190**, 354–367 (2017).
[19]Z. Wang, H. Zhu, D. Zhang, H. H. Goh, Y. Dong, and T. Wu, "Modelling of wind and photovoltaic power output considering dynamic spatio-temporal correlation," Appl. Energy **352**, 121948 (2023).
[20]J. Widen, "Correlations between large-scale solar and wind power in a future scenario for Sweden," IEEE Trans. Sustainable Energy **2**, 177–184 (2011).
[21]D. Liu, C. Wang, F. Tang, and Y. Zhou, "Probabilistic assessment of hybrid wind-PV hosting capacity in distribution systems," Sustainability **12**, 2183 (2020).
[22]C. Draxl, A. Clifton, B.-M. Hodge, and J. McCaa, "The Wind Integration National Dataset (WIND) Toolkit," Appl. Energy **151**, 355 (2015).
[23]E. Wilson, A. Parker, A. Fontanini, E. Present, J. Reyna, R. Adhikari, C. Bianchi, C. CaraDonna, M. Dahlhausen, J. Kim, A. LeBar, L. Liu, M. Praprost, P. White, L. Zhang, P. DeWitt, N. Merket, A. Speake, T. Hong, H. Li, N. Mims Frick, Z. Wang, A. Blair, H. Horsey, D. Roberts, K. Trenbath, O. Adekanye, E. Bonnema, R. E. Kontar, J. Gonzalez, S. Horowitz, D. Jones, R. Muehleisen, S. Platthotam, M. Reynolds, J. Robertson, K. Sayers, and Q. Li, "End-use load profiles for the U.S. Building Stock," Technical Report No. 4520 (DOE Open Energy Data Initiative (OEDI); National Renewable Energy Laboratory (NREL), 2021).
[24]"American National Standard for Electric Power Systems and Equipment—Voltage Ratings (60 Hertz)," ANSI C84.1 (ANSI, New York, 2020).
[25]C. R. Harris, K. J. Millman, S. J. Van Der Walt, R. Gommers, P. Virtanen, D. Cournapeau, E. Wieser, J. Taylor, S. Berg, N. J. Smith, R. Kern, M. Picus, S. Hoyer, M. H. Van Kerkwijk, M. Brett, A. Haldane, J. F. Del Río, M. Wiebe, P. Peterson, P. Gérard-Marchant, K. Sheppard, T. Reddy, W. Weckesser, H. Abbasi, C. Gohlke, and T. E. Oliphant, "Array programming with NumPy," Nature **585**(7825), 357–362 (2020).
[26]F. Pedregosa, G. Varoquaux, A. Gramfort, V. Michel, B. Thirion, O. Grisel, M. Blondel, P. Prettenhofer, R. Weiss, V. Dubourg, J. Vanderplas, A. Passos, D. Cournapeau, M. Brucher, M. Perrot, and E. Duchesnay, "Scikit-learn: Machine learning in Python," J. Mach. Learn. Res. **12**, 2825–2830 (2011).
[27]National Renewable Energy Laboratory, "WRDB (Wind Resources DataBase)" [online], https://wrdb.nrel.gov/ (accessed 01-Feb-2025).
[28]National Renewable Energy Laboratory, "National Solar Radiation Database (NSRDB)" [online], https://nsrdb.nrel.gov/ (accessed 01-Feb-2025).
[29]A. P. Dobos, "PVWatts Version 5 Manual," Technical Report No. NREL/TP-6A20-62641 (National Renewable Energy Laboratory (NREL), Golden, CO, 2014).
[30]M. Hünnebeck *et al.*, "windpowerlib documentation" [online]. https://windpowerlib.readthedocs.io/ (accessed 01-Feb-2025).
[31]National Renewable Energy Laboratory, "Open Energy Data Initiative (OEDI)" [online], https://www.nrel.gov/data/oedi.html (accessed 01-Feb-2025).
[32]Electric Power Research Institute, "OpenDSS: The Open Distribution System Simulator" [software], https://www.epri.com/pages/sa/opendss (accessed 01-Feb-2025).
[33]B. Palmintier and B. Hodge, "SMART-DS: Synthetic models for advanced, realistic testing—Distribution systems and scenarios," Advanced Research Projects Agency–Energy (ARPA-E), U.S. Department of Energy, 2017.
[34]J. Wohland, P. Hoffmann, D. C. A. Lima, M. Breil, O. Asselin, and D. Rechid, "Extrapolation is not enough: Impacts of extreme land-use change on wind profiles and wind energy according to regional climate models," EGUsphere **15**, 1–26 (2023).
[35]National Renewable Energy Laboratory (2020). "Bergey Excel 10 8.9 kW (7) — NREL/turbine-models power curve archive," GitHub, https://nrel.github.io/turbine-models/BergeyExcel10_8.9kW_7.html (accessed 23-Jan-2025).
[36]K. S. Anderson, C. W. Hansen, W. F. Holmgren, A. R. Jensen, M. A. Mikofski, and A. Driesse, "pvlib python: 2023 project update," J. Open Source Software **8**, 5994 (2023).